UNITED NATIONS UNIVERSITY
GEOTHERMAL TRAINING PROGRAMME
Orkustofnun, Grensasvegur 9,
IS-108 Reykjavik, Iceland

Reports 2012
Number 31

GEOCHEMICAL AND ISOTOPIC STUDY OF THE MENENGAI GEOTHERMAL FIELD, KENYA

Lawrence Ranka Sekento
Geothermal Development Company, Ltd. – GDC
P.O. Box 17700 – 20100
Nakuru
KENYA
lranka@gdc.co.ke

ABSTRACT

Results of chemical and isotopic investigations of geothermal fluids within the Menengai high temperature geothermal field are presented. The isotopic composition of lakes, boreholes and springs in the Kenyan rift valley, from Lake Naivasha in the South to Lake Baringo in the North are also presented and discussed. The Menengai area is mainly composed of trachytic lavas traversed by north-northwest and north-northeast trending fracture zones with the Ol'Rongai and Molo Tectono volcanic axes, within which there are several eruptive centres. Geochemical samples were collected in the year 2012 from the exploration/production geothermal wells in Menengai and analysed for chemical constituents in GDC and KenGen geochemical laboratories and for stable isotopes of oxygen and hydrogen at the Institute of Earth Sciences, University of Iceland.

In addition, samples for isotope measurements were collected from lakes and cold water shallow boreholes, as well as cold and hot springs and analysed at the Institute of Earth Sciences, University of Iceland. The results indicate that the Menengai thermal fluids are of meteoric origin as they plot close to the local evaporation water line, however mixing of Lake Nakuru and groundwater is seen both in the isotopic and chemical composition of the fluids. In well MW-05 the fluid is richer in ^{18}O, either due to more intense water-rock interaction, or boiling at higher temperature than in wells MW-01 and MW-04. The isotopic composition of the lakes has varied considerably with time, due to changing rainfall patterns, lake water levels and the amount of evaporation over the years. The shallow and cold springs are all of meteoric origin, as they plot in a cluster slightly more enriched than indicated by the intersection between the local rainwater and evaporation lines. Very little geographical difference is observed for the cold groundwater samples. Fluids discharged by wells MW-01 and MW-04 are sodium bicarbonate in nature. The calculated temperatures from solute geothermometers are somewhat lower than measured temperatures. Flashing of the fluids during discharge causes boiling which results in cooling and lowering of the boiling temperature and hence high CO_2 in both MW-01 and MW-04. High CO_2 could also be originating from a degassing magmatic body.

1. INTRODUCTION

Menengai is a major Quaternary central volcano located within the axis of the central segment in the Kenyan Rift. It hosts one of the high-temperature geothermal fields located in the Kenyan rift valley (Figure 1). The age of the youngest eruption episode (~1400 yrs.) indicates the possibility of a still active magma body below the Menengai caldera. Detailed surface exploration was carried out in 2004, with subsequent infill exploration studies being done in 2009, 2010 and 2011. This led to the first exploration well being sunk in 2011 and several wells have been drilled since then. Water is the major substance in the lithosphere implicated in convective heat and mass transfer, and any waters or aqueous fluids in geologic systems are involved in many chemical reactions. Knowledge of the origin of water is fundamental to understanding geothermal reservoirs. Isotopic composition of water provides a recognizable signature. During the passage of water through aquifers, the hydrogen isotope composition of the water is essentially a conservative property.

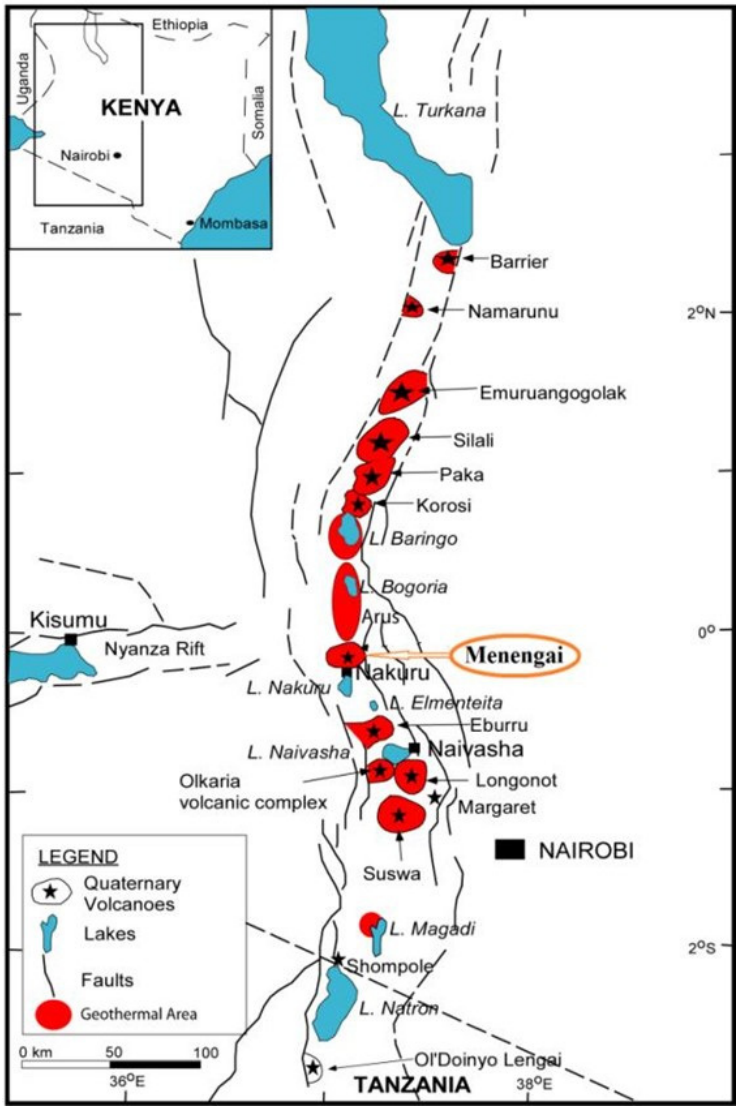

FIGURE 1: Location of Menengai geothermal field in the East African Rift System (obtained from Kipng'ok, 2011)

For this study 25 samples from thermal springs, ambient springs, lake waters, shallow boreholes, thermal wells and gas condensates were collected in Kenya and measured for oxygen and hydrogen isotopes at the Institute of Earth Sciences (IES), Iceland. Chemical data from well water and the steam portion from deep high temperature wells in Menengai geothermal field, Kenya, analysed at both GDC and KenGen geochemical laboratories, are also interpreted in this report. An attempt is made to obtain information on the thermal fluid flow, to classify waters and to study the mixing processes using the geochemical and isotopic composition of the waters.

2. MENENGAI GEOTHERMAL FIELD

2.1 Location

The Menengai geothermal field is located within the Menengai caldera and parts of the Ol' Rongai and Solai areas. Menengai caldera is typified by complex tectonic activity associated with the rift triple junction. This is a zone at which the failed rift arm of the Nyanza rift joins the main Kenyan rift (Figure 1).

2.2 Geology

Two tectono-volcanic axes (TVAs), Molo and Solai, converge at the Menengai caldera (Figure 2) and are important in controlling the geothermal system. Numerous normal faults trending north-northwest form the greater Molo TVA, where eruption centres are also observed and volcanic eruptions have taken

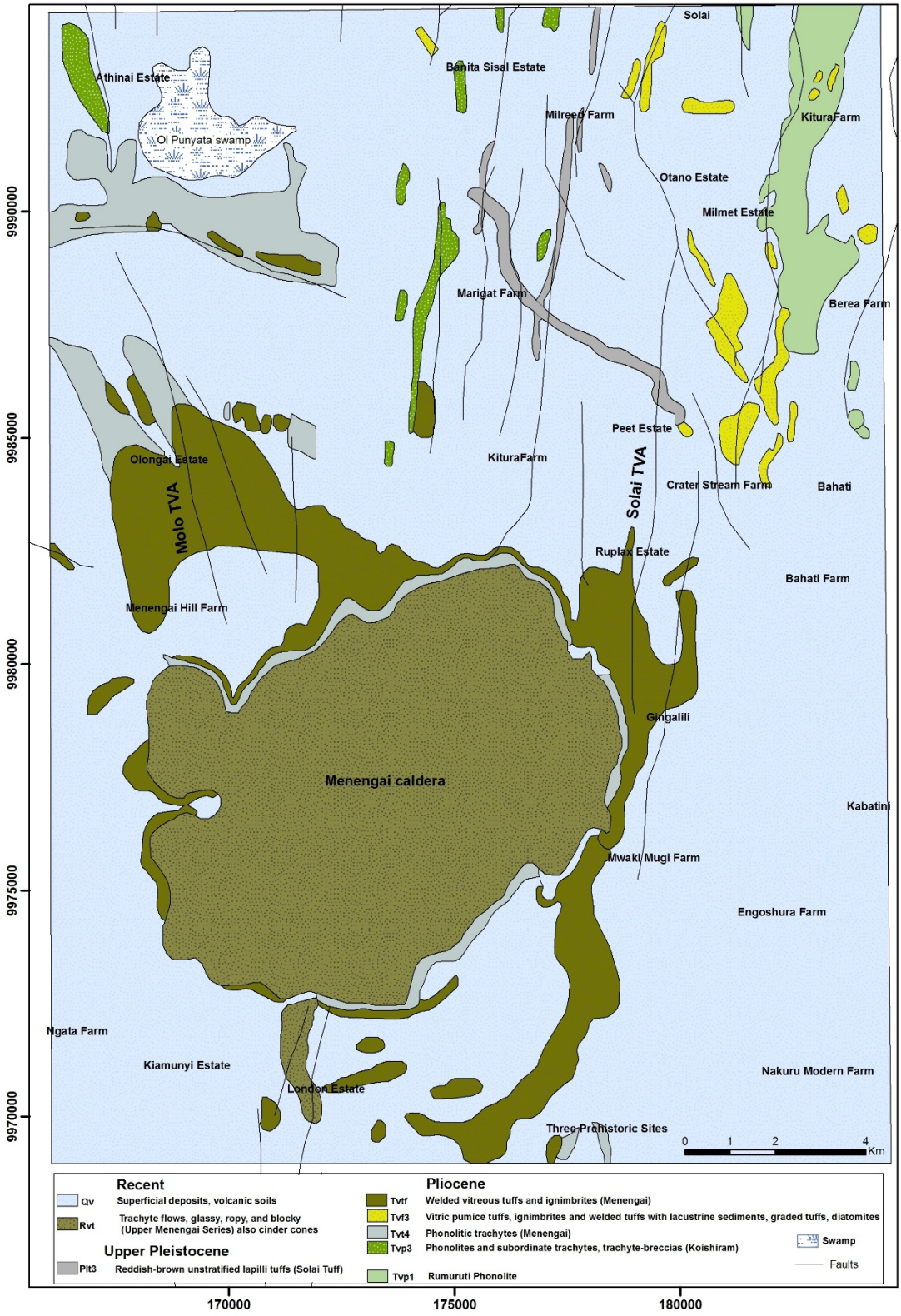

FIGURE 2: Geological and tectonics map of Menengai area

place (Figure 3). The Solai tectonic axis is a narrow graben that runs in a N-S direction from the eastern end of the Menengai caldera through Solai. It is comprised of numerous fault/fracture systems trending N-S (Lagat et al., 2010; Mungania et al., 2004). In the regional set-up, the Molo TVA structure extends northwards through Lomolo, the Goitumet volcanic centre, along the east side of Lake Bogoria to as far as southeast of Lake Baringo. At Ol'Rongai, the structure is marked by intense volcanic activity including explosive (pumice issuing) craters. This part of the structure is adjacent to the Menengai caldera and possibly extends into and through the caldera (Lagat et al., 2010). Geophysical surveys show that a distinct low-resistivity anomaly (<15 Ωm) occurs in the Menengai caldera and extends into the Ol'Rongai area to the northwest part of Menengai geothermal field, presenting a heat source inclining in the same direction as the Molo TVA. Gravity and seismology studies of the Menengai area identified a body, suggested to be a magma chamber that could constitute the heat source, directly beneath the caldera (Simiyu and Keller, 1997; 2001).

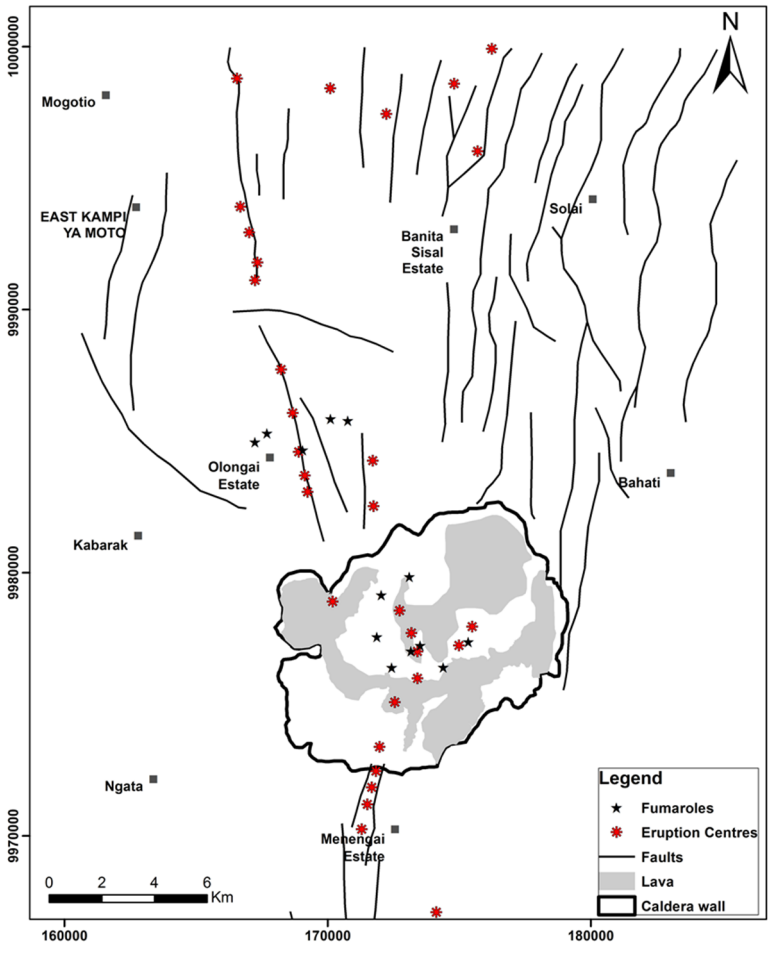

FIGURE 3: Hydrothermal activity in Menengai geothermal field

Most of the area around the caldera is covered mainly by pyroclastics erupted from volcanic centres. Young lava flows, infilling the main caldera, are of Holocene age. Older (Pleistocene) lavas, mainly trachytic in composition, are exposed in the northern parts and are overlain by eruptives from Menengai volcano (Figure 2, Mungania et al., 2004).

The surface drainage is from the eastern and western rift scarps. On the rift floor, the drainage is mainly from Menengai caldera northwards with the exception of drainage from the southern inclines of the Menengai caldera into Lake Nakuru. Surface permeability in the Menengai caldera is high since no surface outflow out of the caldera is observed. The permanent rivers are Molo and Rongai in the northwest part of the area. The crater and Olbanita streams in the eastern parts of the area have water flowing most months of the year. The N-S trending fault/fracture systems provide underground channels resulting in stream water disappearing underground in some places (Lagat et al., 2010). Other surface water bodies around the Menengai geothermal field include Lakes Nakuru and Lake Solai, and the Olbanita swamp, as well as Lakes Baringo and Bogoria further to the north. The area lies on the rift floor that gently slopes northwards.

2.3 Hydrothermal activity

Hydrothermal activity in Menengai geothermal field is manifested in the form of fumaroles, warm/ambient temperature boreholes, and altered grounds. Fumaroles are located mainly inside the caldera floor and over the Ol'Rongai area (Figure 3). The steam from these fumaroles has a very strong

H_2S gas smell, and at some solfataras (Mungania et al., 2004) deposition is evident on the surface as well as extensively altered pumiceous formation in the caldera. However, the fumaroles are not very strong. The structural controls for these fumaroles appear to be the eruption centres and or buried faults. All the fumarole vents are marked by silica and/or chalcedonic deposition (Mungania et al., 2004). At the Ol'Rongai area, the fumaroles are characterised by low–pressure steam and alteration of the grounds where silica deposition is observed. Soft altered, hot to warm grounds are also observed.

3. METHODOLOGY

3.1 Natural isotopes

The isotopic composition of oxygen and hydrogen are reported in terms of differences of $^{18}O/^{16}O$ and D/H ratios relative to the Standard Mean Ocean Water (SMOW). The ocean, being the largest water reservoir and relatively homogeneous, was chosen as the reference standard for the δ scale of both oxygen and hydrogen isotopes in water samples (Craig, 1961a). The isotopic composition is expressed as per mil difference relative to SMOW. The δ-(per mil) value is defined as:

$$\delta‰ = \left[\frac{R_{sample}}{R_{SMOW}} - 1\right] \times 1000 \quad (1)$$

where R is the atom ratio D/H and $^{18}O/^{16}O$, e.g. for hydrogen:

$$\delta D = \left[\frac{(D/H)_{sample} - (D/H)_{SMOW}}{(D/H)_{SMOW}}\right] \times 1000 \quad (2)$$

Positive values of $\delta^{18}O$ and δD thus signify enrichment of the isotope species relative to the standard (SMOW), whereas negative values imply depletion of those isotopes in the sample relative to the standard.

Isotope fractionation is a consequence brought on because certain thermodynamic properties of molecules depend upon their atomic masses. Thermodynamic properties of isotopic molecules have been studied extensively by Urey (1947) and Bigeleisen (1952) among others. Because of the existence of three stable isotopes of oxygen and two of hydrogen, ordinary water molecules have nine different configurations whose masses are given by their mass numbers. The vapour pressures of the different isotopic molecules of water are inversely proportional to their masses. Therefore, $H_2{}^{16}O$ has a higher vapour pressure than $D_2{}^{18}O$, and for this reason, water vapour formed by evaporation of water is enriched in ^{16}O and H while the remaining water is enriched in ^{18}O and D. Previous studies by Gat (1996) have shown that isotope fractionations that accompany evaporation from the ocean and other surface waters and the reverse process of rain formation account for the most notable changes. Local annual means for precipitation have been established and Craig (1961b) showed that a meteoric line describing the relationship between δD and $\delta^{18}O$ applies all over the world, although deviations are known and local lines have been described. Geothermal water values suggest its origin, but mixing, water-rock interaction, condensation and age may have to be accounted for (Ármannsson, 2011). The $\delta^{18}O$ and δD values of meteoric water are linearly related and can be represented by an equation: The line defined by Equation 3 is termed the "World Meteoric Water Line" (WMWL), and is based on precipitation data from locations around the globe.

$$\delta D = 8\,\delta^{18}O + 10 \quad (3)$$

In Kenya, isotope studies were mainly done in the 1980s. This includes oxygen and hydrogen isotopes of precipitation with emphasis on Lake Naivasha (close to the Olkaria geothermal field) and its lowering water level at the time, and Lake Baringo, the only fresh water lakes in the rift. Application of isotope hydrological methodologies and isotope hydrological investigations of thermal waters of the Kenya Rift

Valley have been done since the 1970s. A local meteoric waterline, the origin, and the recharge areas of the thermal waters in the south rift have been reported (Allen et al., 1987).

In Kenya, data from rainfall samples were used to identify the local meteoric waterline, (Kenya Rift Valley Meteoric Water Line, KRML), with a correlation coefficient of 0.94 (Allen et al., 1987):

$$\delta D = 5.56\,\delta^{18}O + 2.04 \quad (4)$$

Kenya Rift Valley Evaporation Line (KRVEL) from Ármannsson (1994) is also described:

$$\delta D = 5.49\,\delta^{18}O + 0.08 \quad (5)$$

And Continental African Rain Line (CARL) from Ármannsson (1994):

$$\delta D = 7\,\delta^{18}O + 11 \quad (6)$$

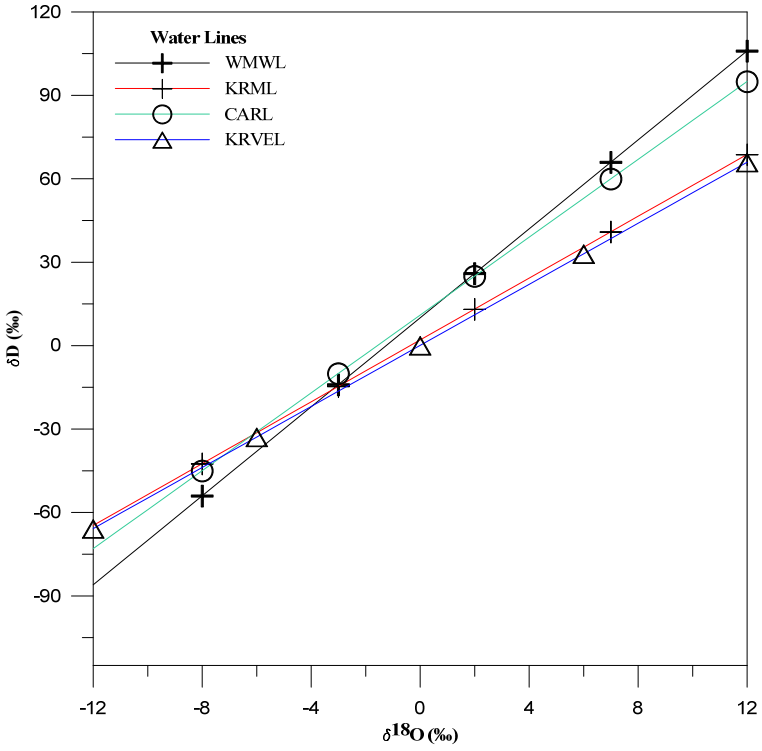

FIGURE 4: World Meteoric Water Line (Craig, 1961), Kenya Rift Valley Meteoric Water Line (Allen, D. J and Darling, W. D., 1987); Continental African Rain Line (Ármannsson, 1994); and Kenya Rift Valley Evaporation Line (Ármannsson, 1994)

The "lines" described by the above equations are shown in Figure 4. The lifetimes of geothermal systems are generally poorly known, as are fluid circulation times. Estimated ages of geothermal systems lie in the range of 0.1 to 1 million years (Arnórsson et al., 2007). Fluid circulations times may range from a few hundreds of years, or even less, to more than 10,000 years in geothermal systems (Arnórsson et al., 2007; Sveinbjörnsdóttir et al., 2004). The origin of fluids in geothermal systems is essentially meteoric water or seawater or mixtures thereof. The origin of the water discharged by volcanoes and hot springs may be partially juvenile and derived from the upper mantle of the earth. Its isotopic composition is probably determined by the kind of rocks of the upper mantle, and it is changed not only by an exchange with crustal rocks over a wide temperature range but also by being mixed with meteoric water, or sea water trapped in the rocks. Previous studies by Craig (1963) showed that $\delta^{18}O$ values of hot water and steam discharged from geothermal areas are variable, while δD values remain nearly constant. Craig attributed the oxygen-isotope shift to gradual equilibration of oxygen in the water with silicate and carbonate rocks. The reaction is temperature dependent such that an increase in temperature allows the $\delta^{18}O$ value of the water to approach that of the rocks, and vice versa. However, reactions of rocks with seawater or reservoir water at low to intermediate temperatures can cause a less common shift of $\delta^{18}O$ away from the meteoric water line towards more negative values, as Nicholson (1993) showed (Figure 5). The δD values of geothermal waters remain unchanged, mostly because the hydrogen content of silicate and carbonate rocks is low compared to that of water, but the little variation is attributed to isotope exchange with hydrocarbons, hydrogen sulphide, and hydrated minerals such as clays (Ellis and Mahon, 1977).

3.1.1 Oxygen and hydrogen isotopes in geothermal investigations

Oxygen and hydrogen isotopes are widely used in geothermal studies. They are extensively applied to determine the origin and history of geothermal fluids and most often serve as natural tracers for the provenance of geothermal water. An important aspect of geothermal investigations is to determine the recharge to the geothermal systems that is essentially of meteoric origin. Ground waters derived from shallower depths often have isotope compositions that are consistent with local meteoric precipitation. Deep drilling for geothermal energy has provided important information on the sources and composition of geothermal fluids, their reaction with rock-forming minerals, the migration of the fluid, and fluid phase separation and fluid mixing processes (Arnórsson et al., 2007).

3.2 Classification of thermal waters

3.2.1 Cl-SO_4-HCO_3 ternary diagram

Giggenbach (1991) proposed a Cl-SO_4-HCO_3 ternary diagram for the initial classification of geothermal solutions to identify whether geothermometers are applicable for the given water sample, as most solute geothermometers work only for neutral waters. According to Giggenbach (1991), solute geothermometers can only be applied to what is referred to as "mature waters", characterized by high Cl and low SO_4. This diagram is also helpful in providing an initial indication of the mixing relationships or geographic groupings.

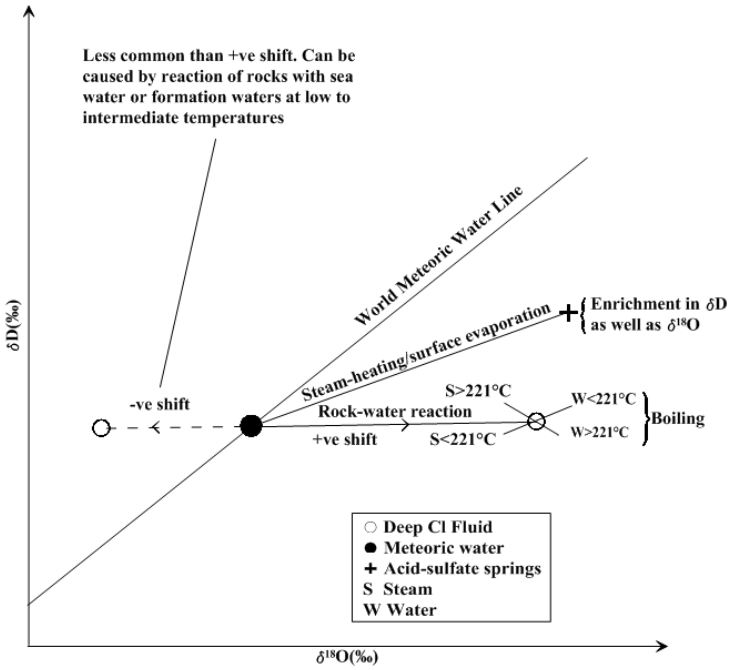

FIGURE 5: Schematic diagram showing trends in isotopic signatures of meteoric water and geothermal fluids with active processes (Nicholson, 1993)

3.2.2 The Na-K-Mg ternary diagram

The Na-K-Mg ternary diagram is used to classify waters into fully equilibrated, partially equilibrated and immature waters. It can also be used to predict the equilibrium temperature and also the suitability of thermal waters for the application of ionic solute geothermometers. It is based on the temperature dependence of the full equilibrium assemblage of potassium and sodium minerals (Giggenbach, 1988). The use of the triangular diagrams is based on the temperature dependence of K^+, Na^+ and Mg^{2+} cations in geothermal fluids. If a data point plots on or above the full equilibrium line, the diagram shows attainment of equilibrium.

3.3 Geothermometry

Equilibria between minerals, geothermal solutions and, in some cases, a vapour phase can affect the chemical composition of geothermal fluids, providing the basis for chemical geothermometry. An assumption is, therefore, made that this equilibrium is attained in the reservoir by the geothermal fluids. Chemical geothermometers are normally applied to thermal springs, steam vents, and geothermal wells for inferring reservoir temperatures in geothermal exploration and exploitation. The most widely used geothermometers are based on silica concentrations, cation ratios (mainly Na/K), and gas ratios and concentrations in the steam phase.

3.3.1 Silica geothermometers

Silica geothermometers assess reservoir temperatures from the silica content of natural water in equilibrium with either quartz or chalcedony. Temperatures predicted by these geothermometers are referred to as quartz and chalcedony temperatures, respectively (Arnórsson, 2000a). The quartz geothermometers work best for waters in the subsurface temperature range of 120-250°C (Arnórsson, 2000b). The basic reaction for the dissolution of silica minerals is:

$$SiO_{2(S)} + 2H_2O = H_4SiO_{4(aq)} \quad (7)$$

Therefore, very high pH levels can lead to overestimation of the reservoir temperature if aqueous speciation of silica is not considered. At pH levels below ~9, nearly all dissolved silica is present in a solution as undissociated silicic acid, $H_4SiO_2^-$. At higher pH levels, the silicic acid dissociates to form $H_3SiO_4^-$, thus, effectively increasing the solubility of silica in water in equilibrium with quartz. The silica geothermometer equations used to calculate the temperature of a reservoir are as follows:

Quartz, no steam loss, temperatures between 25 and 250°C (Fournier, 1977):

$$T°C = \frac{1309}{5.19 - \log S} - 273.15 \quad (8)$$

Quartz, 0-350°C (Arnórsson, 2000c):

$$T°C = -55.3 + 0.26590\,S - 5.3954 \times 10^{-4}S^2 + 5.5132 \times 10^{-7}S^3 + 74.360 \log S \quad (9)$$

The silica geothermometer is based on several assumptions: the fluid is in equilibrium with quartz/chalcedony in the reservoir; the vapour pressure of pure water fixes the pore fluid pressure in the reservoir; there is no mixing of hot and cold water during up flow; and lastly there is either conductive cooling of the ascending water or adiabatic cooling with steam separation at 100°C (Fournier, 1991).

3.3.2 Cation geothermometers

Cation geothermometers are commonly used to estimate reservoir temperatures. Of the cation geothermometers, the Na-K geothermometer is the most widely used geothermometer. The partitioning of sodium and potassium between aluminosilicates and aqueous solutions is strongly temperature dependent. This is generally interpreted to be a result of equilibrium between Na and K feldspars and the aqueous solution, described by the reaction:

$$K^+ + \textit{Na-feldspar} = \textit{K-feldspar} + Na^+$$

Based on this principle, various Na/K cation geothermometers have been developed (e.g. Fournier and Truesdell, 1973). Recently, a new Na/K geothermometer was developed purely on an empirical basis and calibrated from field data (Can, 2002). The cation geothermometers considered in this study are listed below; *Na* and *K* refer to the concentrations of these cations in solution in mg/kg:

Arnórsson et al. (1983), 250-350°C:

$$T°C = \frac{1319}{1.699 + \log\left(\frac{Na}{K}\right)} - 273.15 \quad (10)$$

Giggenbach et al. (1988):

$$T°C = \frac{1390}{1.75 + \log\left(\frac{Na}{K}\right)} - 273.15 \quad (11)$$

3.3.3 Gas geothermometers

Gas geothermometers are based on gas equilibria with an assumption that the gas is in equilibrium with the thermal water and the bedrock. The concentrations and ratios of many gas species are sensitive functions of the reservoir temperature. Thus, gas equilibrium develops and determines the relative concentration of the gas species, assuming that chemical equilibrium does exist among the various species at depth in the reservoir (D'Amore, 1991). Boiling generally increases geothermometer temperatures in the early stages because gas preferentially partitions into the vapour phase where gaseous species partially react (Nehring and D´Amore, 1984). In 1986 Arnórsson developed a method for correcting for the effects of steam condensation. Geothermometers based on ratios are not affected by steam condensation (Arnórsson, 1998). In this study the following gas geothermometers were used (Q is the gas concentration in log mmol/kg):

Arnórsson and Gunnlaugsson (1985), all waters:

CO_2 $$T°C = -44.1 + 269.25Q - 76.88Q^2 + 9.52Q^3 \quad (12)$$

Arnórsson and Gunnlaugsson (1985), waters >300°C:

H_2S $$T°C = 246.7 + 44.81Q \quad (13)$$

Arnórsson and Gunnlaugsson (1985), waters in the range 200°C-300°C and Cl >500 ppm:

CO_2/H_2 $$T°C = 341.7 - 28.57Q \quad (14)$$

H_2 $$T°C = 277.2 + 20.99Q \quad (15)$$

H_2S/H_2 $$T°C = 204.1 - 39.48Q \quad (16)$$

3.4 Mineral saturation

Various aqueous species in geothermal fluids form when ions and compounds are dissolved in water. The relationship between aqueous species is expressed by the equilibrium constant (K). Evaluation of chemical equilibria between minerals and aqueous solutions in natural systems requires the determination of the activities of aqueous species and knowledge of the solubilities of the minerals present in the bedrock. Assumption of specific mineral-solution equilibria is necessary when applying geochemistry to obtain an understanding of various physical features of a geothermal system. The saturation index of several minerals is computed as a function of temperature and if the saturation indices of the minerals converge to zero (saturation) at a specific temperature, that temperature is taken to represent the reservoir temperature. However, it is to be noted that care should be taken in interpreting the results of multi-mineral/solute equilibria as the results depend on both the thermodynamic data base used for mineral solubilities and the activities of end-member minerals in solid solutions (Tole et al., 1993).

In this study, the WATCH chemical speciation program (Arnórsson et al., 1982), version 2.4A (Bjarnason, 2010), was used to calculate aquifer water compositions from the analytical data for some water and steam samples collected at the wellhead. The saturation indices (SI) of minerals in aqueous solutions at different temperatures were computed as:

$$SI = \log\frac{Q}{K} \quad (17)$$

where Q is the calculated ion activity product (IAP) and K is the equilibrium constant.

The SI value for each mineral is a measure of the saturation state of the water phase with respect to the mineral phase. Values of SI greater than, equal to, and less than zero represent supersaturation, equilibrium and undersaturation, respectively, for the mineral phase with respect to the aqueous solution.

The minerals anhydrite, quartz, calcite and amorphous silica are normally checked for saturation as these are the minerals that cause scaling in well bores and therefore need monitoring.

4. SAMPLING AND ANALYTICAL METHODS

Water sampling and analysis are essential in the characterization of geothermal fluids and the evaluation of the energy potential of geothermal fields. Chemical analysis also provides good indicators for monitoring reservoir changes in response to production and on the origin of the thermal water as reflected in the water isotopes. Sample collection is critical in order to obtain good quality results and is, therefore, a key process in geochemical activities for evaluating geothermal resources and reservoir management. All the water and steam samples from wells MW-01 and MW-04 used in this study were sampled by staff at GDC. Below is a description on how the samples were collected and treated.

4.1 Sampling

In this study water and gas phase fluid samples from two discharging wells, MW-01 and MW-04, were considered for chemical compositions. Water isotopic compositions for the three wells (MW-01, MW-04 and MW-05) were also considered. The gas portion of well MW-04 was also considered for isotopes. Steam and water samples were collected using the Webre separator at the wellhead as described by Ármannsson and Ólafsson (2006). The water samples were cooled during sampling by passing them through a stainless steel coil immersed in cold water and then the samples were collected into plastic bottles. Steam samples were collected into weighed, evacuated double port glass sampling flasks (Giggenbach bottles) containing 50 ml of 40% w/v NaOH solution. Water samples were collected and preserved accordingly, depending on the type of analysis to be done. Raw untreated samples were collected in 500 ml bottles for determination of pH, conductivity, total dissolved solids (TDS), CO_2 and isotopes. Onsite analysis for H_2S was carried out on the same sample. Filtered untreated samples for Cl, F and B (anions) were collected into 200 ml bottles. Raw untreated samples for silica analysis were also collected in 200 ml bottles and diluted ten times. Samples for cations and SO_4 analysis were filtered through a 0.45 μm millipore membrane; 1 ml of concentrated nitric acid and 1 ml of 0.2 M zinc acetate solution was added to the samples for cation and sulphate analysis (fix sulphides), respectively.

4.2 Analytical methods

All the analytical work on major and trace elements was carried out at GDC and Olkaria geochemical laboratories. Analytical methods for individual components in liquid samples are shown in Table 1.

The isotopic composition of the samples was measured at the Institute of Earth Sciences, University of Iceland, via continuous flow isotope ratio mass spectrometry (CF-IRMS) using a GasBench III headspace analyser coupled to a Delta V CF-IRMS. The room

TABLE 1: Analytical methods used for the different components

Component	Method of analysis
pH	pH meter
Conductivity	Conductivity meter
TDS/	Gravimetry
CO_2	Alkalinity-titration
H_2S	Titration
SiO_2	Spectrophotometry (with ammonium molybdate)
B	Spectrometry
Na	ICP-MS
K	ICP-MS
Ca	ICP-MS
Al	ICP-MS
F	Ion selective electrode
Cl	Ion selective electrode / Spectrophotometry (with thiocyanate)
SO_4	Turbidometry (with barium chloride)
$\delta^{18}O$, δD	Mass spectrometry
Gas samples	Gas chromatography

temperature of the CF-IRMS was kept constant at 19°C. 2 mL of water sample was put into a vial and sealed with a rubber septum. The water samples were first flushed with a gas mixture of 98% He and 2% CO_2 for oxygen isotope measurements and with a mixture of 98% He and 2% H_2 for hydrogen isotope measurements and then allowed to equilibrate with the gas mixture with a constant temperature of 20°C for the Gasbench headspace for 24 hours for oxygen, and for at least 1 hour for hydrogen. Equilibration of hydrogen was facilitated with a platinum catalyst. The samples were then analysed sequentially and calibrated to the Vienna Standard Mean Ocean Water (V-SMOW) using 2 internal standards. The results are reported in permill (‰) V-SMOW ±0.1‰ and ±1‰ for oxygen and hydrogen, respectively.

The very alkaline samples from Lakes Nakura, Bogoria and Elementaita were acidified with 1M HCl to around a pH of 8 prior to oxygen isotope measurements..

5. CHEMICAL AND ISOTOPIC PROPERTIES OF THE FLUIDS

5.1 Isotopic characteristic of the waters

5.1.1 Lakes

Samples were collected for isotopic measurements from 6 lakes on the floor of the Kenya Rift Valley (Figure 6). Furthest south in the study area is Lake Naivasha at an elevation of around 1880 masl. To the north are the smaller lakes: Elementaita (1780 m a.s.l.), Nakuru (1760 m a.s.l.) and Olobosat. Still further north are Lakes Bogoria and Baringo (970 m a.s.l.). Lake Naivasha, Lake Olobosat and Lake Baringo are fresh water lakes while Lake Bogoria, Lake Nakuru and Lake Elementaita are alkaline and high in total dissolved solids (TDS). Lake Naivasha is fed by the perennial rivers Malewa and Gilgil and has been suspected of significant subsurface leakage, probably in both northerly and southerly directions. Darling et al. (1990) demonstrated by stable isotope techniques that lake water was detectable in groundwater at least 30 km south of the lake. It has also been detected in the Eburru geothermal field, northwest of the lake (Darling et al., 1996). Lake Baringo has several permanent water sources in the Perkerra, Molo and Or Arabel rivers, but no surface outlet. It is, however, thought to have a subsurface outlet and seeps into the faulted volcanic bedrock of the rift floor (Dunkley et al., 1993). Due to hydrological conditions, its subsurface outflow is directed exclusively to the north (Allen and Darling, 1992). The highly alkaline lakes are not fed by surface rivers but may have

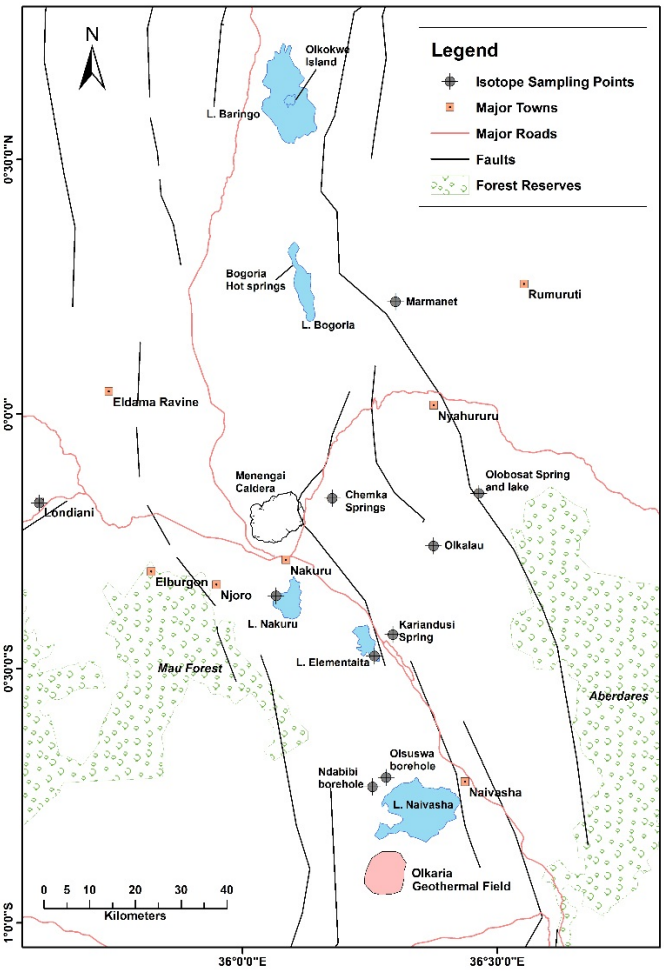

FIGURE 6: Regional sampling points (GDC, 2012)

TABLE 2: Lake, cold springs and thermal waters: isotopic composition (2012)

Lake	$\delta^{18}O$ (‰)	δD (‰)	Temp. (°C)
Nakuru	1.2	18.9	
Elementaita	2.4	21.6	
Bogoria	2.5	29.7	
Olobosat	0.8	7.9	
Naivasha	1.3	10.4	
Baringo	2.6	16.6	
Geothermal well	**$\delta^{18}O$ (‰)**	**δD (‰)**	
MW-01	-0.2	2.6	
MW-04	-0.3	1.0	
MW-04 condensate	-3.0	-15.7	
MW-05	2.5	2.9	
Calculated deep thermal fluid (MW-04)	-1.2	-4.5	
Hot springs	**$\delta^{18}O$ (‰)**	**δD (‰)**	**Temp. (°C)**
Bogoria hotspring	-1.5	-3.0	95
Ol Kokwe island	0.7	3.0	95
Borehole	**$\delta^{18}O$ (‰)**	**δD (‰)**	**Temp. (°C)**
GDC BH-1	-3.3	-12.3	
GDC BH-2	-3.2	-15.2	
Makiki borehole	-3.2	-19.3	
Ndabibi borehole	-2.9	-11.8	
Olsuswa borehole	3.1	20.0	
RVIST borehole	-3.4	-15.9	
Olkalau district hospital	-3.8	-19.0	
Marmanet forest	-3.7	-14.4	
Warm and cold springs	**$\delta^{18}O$ (‰)**	**δD (‰)**	**Temp. (°C)**
Kariandusi spring	-4.0	-19.7	40
Arorwet spring	-3.4	-12.5	21
Kanunga spring	-3.3	-10.4	21
Olobosat spring	-3.4	-14.3	19
Chemka spring	-3.8	-16.8	38

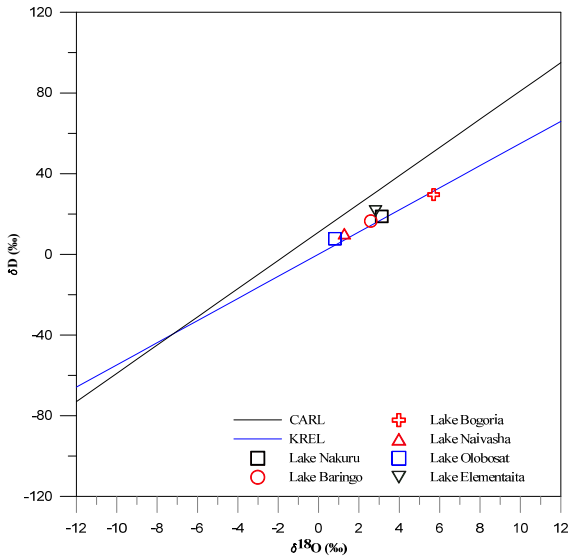

FIGURE 7: δD and $\delta^{18}O$ of Lakes in central Kenya Rift Valley; also shown are the Kenya Rift Evaporation Line (KREL)and Continental African Rain Line (CARL) defined by Ármannsson (1994)

some subsurface leakage. The isotopic composition of the lake samples is shown in Table 2. Their $\delta^{18}O$ and δD values range from 0.8 to 2.6‰ and 7.9 to 29.7‰, respectively, and follow closely the Kenya Rift evaporation line as defined by Ármannsson (1994), shown in Figure 7.

5.1.2 Cold groundwater

The isotopic composition of the cold groundwater around the Menengai area and across the region is represented by eight (8) borehole samples and four (4) samples from cold springs (Table 2). All but one of the samples have similar isotopic characteristics despite the long distances between sample locations. The samples plot in a cluster slightly above the intersection between the local meteoric water line and the Kenya Rift evaporation line, as shown in Figure 8. The borehole Olsuswa, located close to Lake Naivasha is very different from other boreholes. It is isotopically enriched

($\delta^{18}O‰ = 3.06$, $\delta D‰ = 20.02$), suggesting that the origin of the borehole water is mostly lake water. It is however interesting to note that the borehole water is considerably enriched in ^{18}O and D isotopes compared to the present lake value.

5.1.3 Thermal waters

The results of the isotopic measurements of the geothermal fluids are shown in Table 2 and Figure 9 with the locations of the Menengai wells are shown in Figure 10. The water samples range from around -0.32 to 2.48‰ in $\delta^{18}O$ and from 1.04 to 2.87‰ in δD. The steam condensate collected from well MW-04 is more depleted than the water sample due to isotopic fractionation caused by boiling (Table 2). The deep reservoir isotopic fluid composition was calculated from the steam fraction obtained using the WATCH program 2.4 (Bjarnason, 2010) to -1.20‰ and -4.52‰, in $\delta^{18}O$ and δD, respectively. Water samples from wells MW-01 and MW-04 are very similar and plot close to the Kenya Rift evaporation line (Ármannsson, 1994) but the sample from well MW-05 is more enriched in ^{18}O, as demonstrated in Figure 9. This could either be due to more water rock interaction at high temperature or because boiling occurred at higher temperature in well MW-05 than in wells MW-01 and MW-04. The results for the two thermal springs (95°C) collected for this study are also shown in Figure 9. One of them is located on the Ol Kokwe Island in the middle of Lake Baringo. Its isotopic composition, of 0.68‰ in $\delta^{18}O$ and 2.99 ‰ in δD, suggests mixing of shallow ground water with the lake water. This is also the case for the Bogoria hot spring (-1,5‰ and -3.0‰ in δ^{18} and δD, respectively) although it is less influenced by lake water than the Ol Kokwe spring sample.

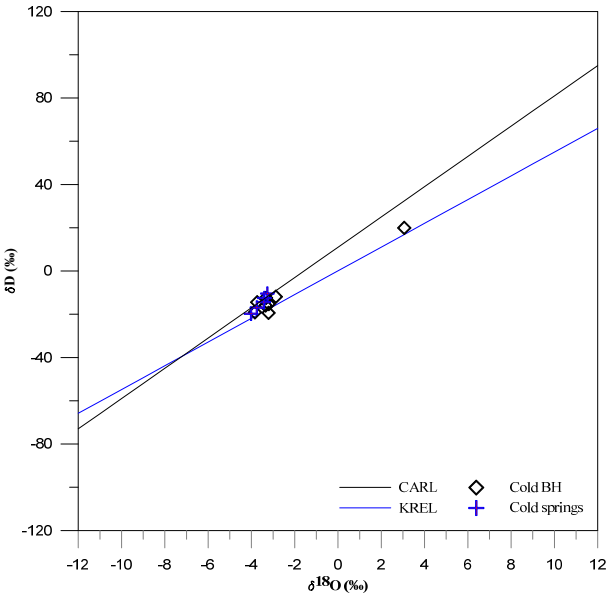

FIGURE 8: δD and $\delta^{18}O$ of cold shallow boreholes (cold BH) and cold springs; the Kenya Rift Evaporation Line (KREL) and Continental African Rain Line (CARL), defined by Ármannsson (1994)

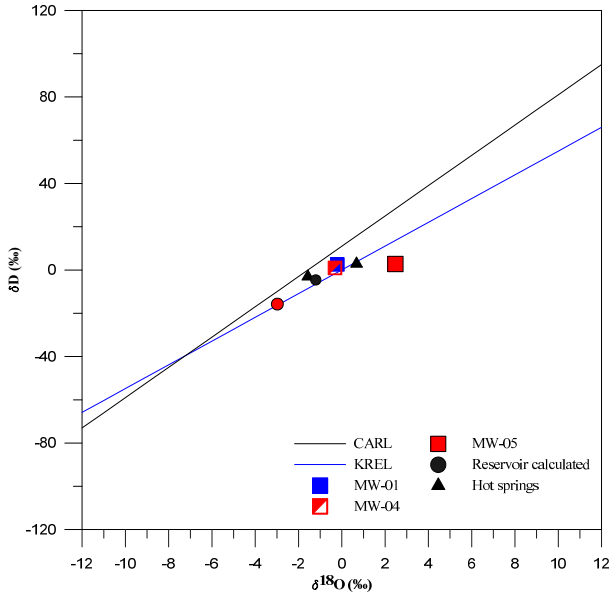

FIGURE 9: δD and $\delta^{18}O$ of thermal waters; the Kenya Rift Evaporation Line (KREL) and Continental African Rain Line (CARL) defined by Ármannsson (1994); the filled red circle are data from well MW-04 condensate

5.2 The chemical characteristics of the thermal water

Representative chemical analyses of the fluids from wells MW-01 and MW-04 are shown in Table 3. The waters of well MW-01 and MW-04 are bicarbonate waters as they plot in the region of high HCO_3, peripheral waters (Figure 11) and low chloride; therefore, the Menengai well fluids are of the Na-HCO_3 type. Waters that plot on the Cl region are usually associated with up flow zones, and are classified as mature waters according to Giggenbach (1991). The low silica suggests that the feed zone is below 200°C and it is decreasing with time during these initial days of discharge. High SO_4 is indicative of low temperature in the feed zone. It is not known whether this is due to effects from drilling fluid lost into the formation.

TABLE 3: Representative chemical composition of the water and steam samples from wells MW-01 and MW-04, Menengai

Date of sampling	Sample ID	Chemical water analysis																		Gas analysis				
		WHP	WSP	H	COND.	TDS	pH / T	B	SO_4	Cl	CO_2	F	H_2S	SiO_2	Ca	Li	Na	K	Mg	Fe	NH_4	CO_2	H_2S	CH_4	H_2	N_2	O_2
		psi	bars	kJ/kg	µΩ/cm	ppm	- / °C	ppm														mmol/kg					
MW-01							20°C																				
29-Jun-11	139	160	0.1	1212	14600	7300	9.2	3.89	271	710	6820	118	37.7	311	1.73	2.54	4201	247	0.143	0.567	15.12	537	12.5	1.1	12.3	1.4	0
15-Aug-11	180	140	0.4	1181	15230	7615	9.2	2.02	242	639	7590	120	12.9	311	2.32	2.58	4427	303	0.209	0.523	19.41	860	11.2	1.0	14.4	2.2	0
5-Sep-11	186	100	0.3	1260	15300	7650	9.3	2.04	245	639	7414	109	17.7	292	2.38	4.90	4424	276	0.229	0.455	na	571	8.7	0.4	7.8	0.9	0
MW-04																											
18-Nov-11	325	82	3.4	1378	11780	7040	9.1/29.4	1.87	358	929.5	5698	151	241.4	411	3.03	0.75	3906	120	0.595	0.581	8.84	1900	34.4	4.4	78.1	16.6	0
1-Dec-11	345	105	3.4	1424	11560	6940	9/24.7	2.99	357	887.5	5588	134	360.4	424	2.65	0.95	3690	149	0.273	0.437	9.74	na	na	na	na	na	na
14-Dec-11	357	150	9.3	1423	10900	6550	8.8/24.9	4.36	241	852.0	5610	141	187.0	344	2.50	0.01	3481	135	0.228	0.636	15.07	1863	28.1	4.9	119.3	26.8	0

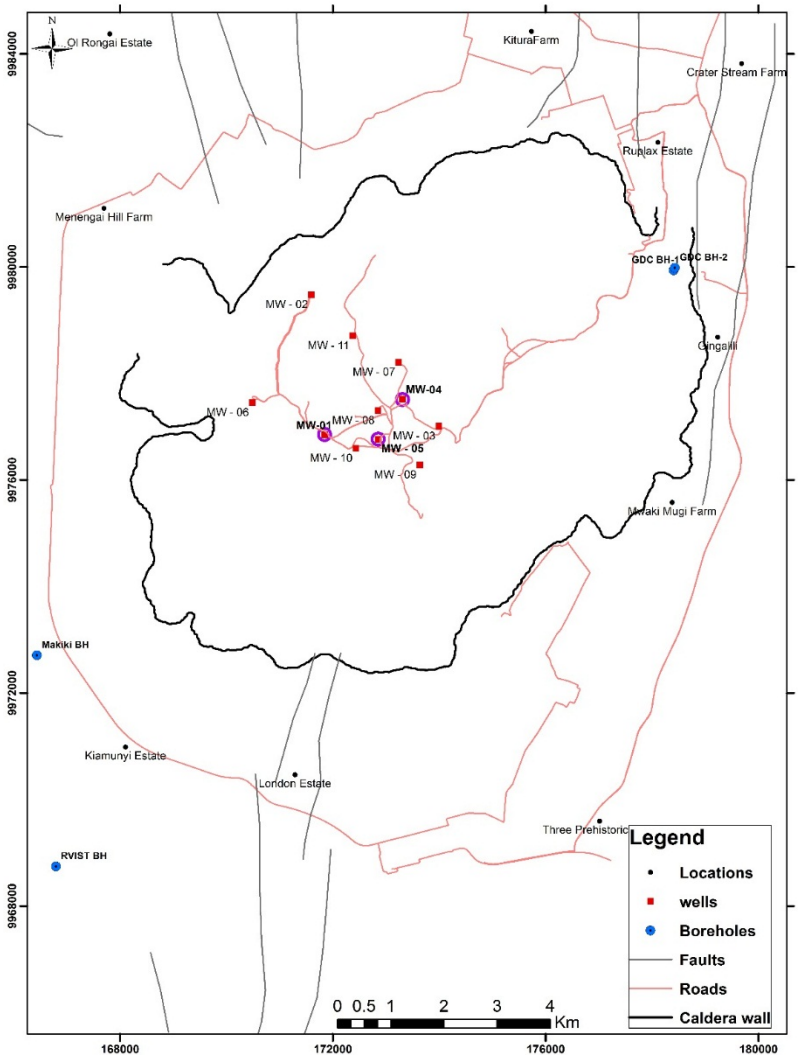

FIGURE 10: Menengai well and shallow borehole sampling locations (GDC, 2012)

Waters from wells MW-01 and MW-04 plot as fully equilibrated waters but, apparently, the Na-K geothermometer is not valid, i.e. equilibrium between Na and K-feldspars does not prevail in the formation. This is demonstrated by the low Na-K temperature reflected in Figure 12, as compared to the measured temperatures.

5.3 Geothermometry

All chemical geothermometers, gas and water, are based on the assumption that temperature dependent mineral solute equilibrium is attained in the geothermal reservoir. In this study, chemical geothermometers of fluids from wells MW-01 and MW-04 were used to assess the reservoir temperatures of the Menengai geothermal field. The ionic balance of the available data is quite reasonable. The results of the geothermometers are shown in Table 4. The Na-K geothermometer for well MW-01 ranges between 160 and 180°C, the quartz geothermometers give temperatures between 171 and 183°C, while the gas geothermometers give the highest temperatures, between 291 and 332°C. For well MW-04 the results are in the range 120-153°C for the Na-K geothermometer, ~202°C for the

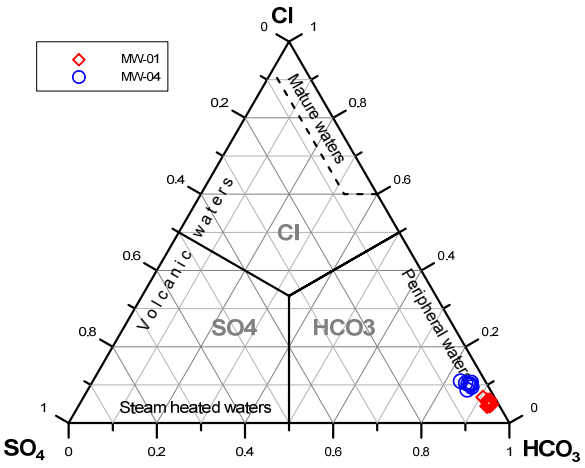

FIGURE 11: Plot of relative Cl-SO_4-HCO_3 components of wells MW-01 and MW-04

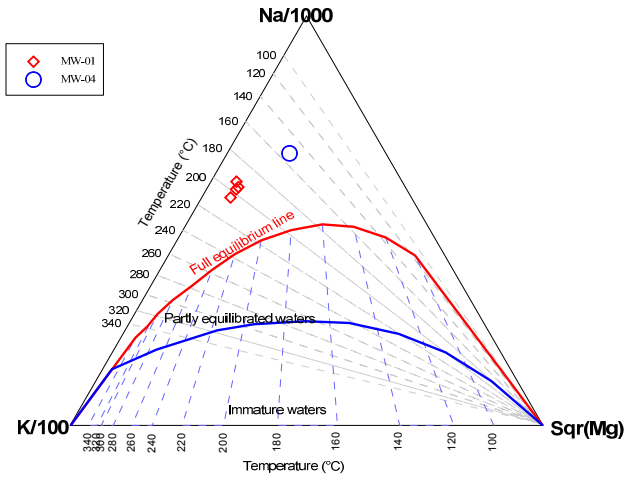

FIGURE 12: Plot of relative Na-K-Mg components of wells MW-01 and MW-04

quartz geothermometers and 302-334°C for the gas thermometers. The Na-K geothermometers are not valid, i.e. equilibrium between Na and K-feldspars does not prevail in the formation, as demonstrated by the low Na-K geothermometer temperatures.

TABLE 4: Results of solute and gas geothermometers used on fluids from wells MW-01 and MW-04, Menengai

Date of sampling	Sample ID	T Na/K[a]	T Na/K[b]	T Qtz[a]	T Qtz[b]	T CO_2	T CO_2/H_2	T H_2S/H_2
MW-01								
29-Jun-11	139	160	177	173	176	323	295	304
15-Aug-11	180	171	187	179	183	332	291	308
5-Sep-11	186	164	181	171	173	320	289	302
MW-04								
18-Nov-11	325	120	137	202	202	334	302	318
1-Dec-11	345	136	153	201	201	325	302	321
14-Dec-11	357	134	151	201	201	281	308	329

T Na/K (a & b): Arnórsson et al. 1998 & 1983, respectively;
T Qtz (a & b): Fournier and Potter, 1982, Arnórsson et al. 1988, respectively; and
Gas: Arnórsson and Gunnlaugsson, 1985.

5.4 Reservoir temperature and pressure profiles

Figure 13 shows the temperature and pressure logs for well MW-04 during heating and discharge. The production casing of MW-04 is set at 1100 m. From these logs it is possible to locate the probable aquifers/feed zones. These compared well with the loss of drilling fluid circulation. There is a major feed zone at a depth between ~1600 and 1800 m with another one being encountered at ~1400 m. The production is from the aquifer at ~1800 m and may be at an even shallower depth. The zone (1600-1800 m) was still extensively cooled when the well was first discharged. Discharging, the well is boiling from the producing aquifer at 1800 m. At ~2050 m depth the temperature is measured ~390°C. The high bottom temperature both during heat up and discharge is most likely a non-porous layer below the lowest aquifer in the well. During drilling it got little cooling and is, therefore, fast to recover. During discharge, the bottom section is not disturbed by the inflow above and therefore maintains a high temperature close to the formation temperature.

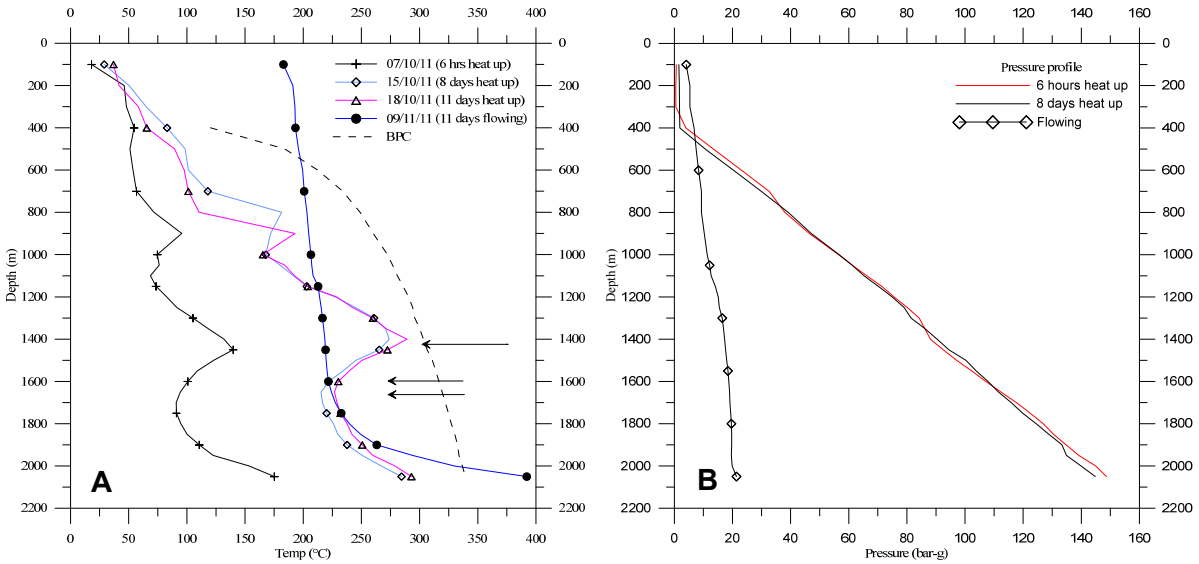

FIGURE 13: Well MW-04, a) temperature profiles, b) pressure profiles; arrows indicate feed zones

5.5 Mineral saturation

Figure 14 shows a plot of the saturation index, log Q/K, calculated from well MW-04 liquid. The liquid is supersaturated with respect to calcite but undersaturated with respect to anhydrite, amorphous silica, and quartz, although quartz becomes slightly oversaturated below 200°C. Convergence of equilibrated minerals to log (Q/K) = 0 does not occur in the temperature range shown here. The selection of more minerals such as actinolite, wollastonite, epidote, pyrite, albite, K-feldspar might be helpful in finding the equilibrium temperature which is likely to be a higher temperature, as indicated by the measured temperature (Figure 13a).

6. DISCUSSION

Isotopic compositions of three of the lakes studied can be compared to earlier isotopic measurements published by Darling et al. (1990), Tiercelin et al. (1987) and Cioni et al. (1992). Dramatic changes were observed with time in the lakes, as demonstrated in Table 5 and Figure 15. The range in $\delta^{18}O$ of Lake Baringo with time is about 6‰ and the change in δD is 30‰. The sample from1988 is similar to the 2012 sample, whereas the samples from 1986, 1989 and 1991 are much more enriched. This is also the case for the 1986 isotope enriched sample from Lake Naivasha and the earlier samples from Lake Bogoria (Figure 15).

This shows that there have been climatic changes with periods of high and low rainfall and different amounts of evaporation from the lakes and, hence, different lake levels. Lake levels can contribute towards explaining the observed isotopic differences, in that samples from shallow water are likely to have experienced more evaporation. Lakes Nakuru and Elementaita contain large concentrations of Na^+, HCO_3^- and CO_3^{2-} ions, as they are water sumps, with no observable outflows (Dunckley et al., 1990). However, the waters are still of meteoric origin and plot on the local evaporation line.

Plotted in Figure 16 are earlier results from Darling et al. (1990) on Lakes Baringo and Naivasha, as well as Tiercelin et al. (1987) and Cioni et al. (1992) for Lake Bogoria. All follow closely the Kenya rift evaporation line, but are more enriched than the present results. Shallow cold water boreholes are of meteoric origin, as well as the cold springs and fall close to the intersection of the Continental African Rain Line and Kenya Rift Evaporation Line. Despite the long distances between the boreholes and springs, very little isotopic variations are observed, except for one borehole, Olsuswa, located close to

Lake Naivasha, which is more enriched in 18O and D than the present value for the lake and therefore reflects the former isotopic composition of the lake. This suggests an outflow from Lake Naivasha in a northwest direction. It is however important to note that the lake water is not observed in the neighbouring Ndabibi borehole; this also shows how the groundwater flow is fissure controlled. Thermal water from Menengai wells MW-01, MW-04 and MW-05 is of meteoric origin, with oxygen shift being observed in well MW-05, probably due to water rock interaction at higher temperatures. Input from Lake Nakuru is suggested on the basis of high concentrations of Na and HCO3 in the well fluids, and on isotopic composition. The ratio of the two components is, however, difficult to determine as the isotopic and presumably the chemical composition of the lakes vary with time, and the lake water influencing the wells is a mixture of present and older lake water. If the present value for Lake Nakuru is used as the lake end-member, the mixture is 20% lake water and 80% groundwater. The two hot springs studied, Ol Kokwe hot spring within the Boringo fresh lake, and the Bogoria hot spring at the shore of the saline Lake Bogoria are both influenced by the respective lake waters. Lake Bogoria hot spring is very similar in isotopic composition to that of the calculated deep Menengai reservoir.

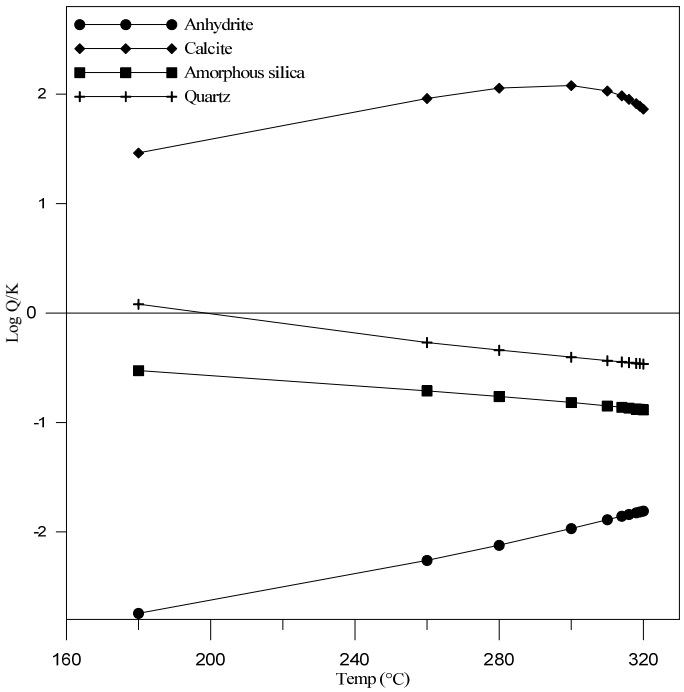

FIGURE 14: Graph showing log Q/K vs. T for well MW-04 fluid

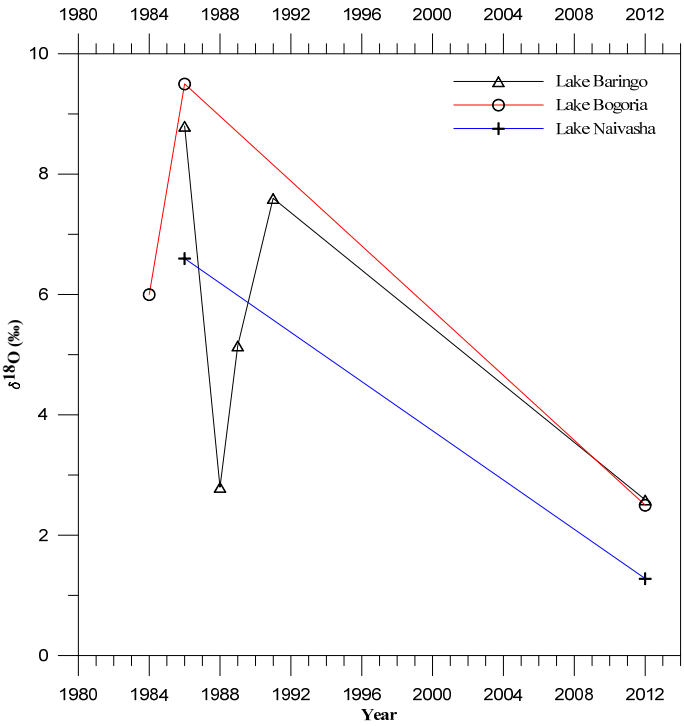

FIGURE 15: Kenya Rift Valley lakes, changes in isotopic composition with time

The isotopic composition of the geothermal water within the Olkaria geothermal field is well documented (Darling et al., 1990). For comparison, the results from Olkaria are shown in Table 5 and in Figure 16. The fluids circulating in the Olkaria geothermal field have been interpreted to be a mixture of local cold groundwater and Lake Naivasha in a ratio of 1:2, as described by Darling et al. (1990), with the Olkaria Northeast field being influenced the most (Figure 16).

The Na-K-Mg ternary diagram (Figure 12) gives a clue as to whether geothermal water samples have been affected by mixing with groundwater. Mixing of cooler inflows from shallower aquifers with hotter fluids from deeper feeds in the well is possible as indicated by the low quartz and Na/K equilibrium temperatures relative to the measured temperatures.

TABLE 5: Isotopic compositions of Lakes and Olkaria thermal wells; the a, b, c, d and e superscripts indicate the year of sampling, 1986, 1988, 1989, 1991, and 1984, respectively. Previous samples by Darling et al. are indicated by *, Tiercelin et al. (1987) by ♦, and Cioni et al. (1992) by •

Lake	$\delta^{18}O$ (‰)	δD (‰)
*Naivasha[a]	6.6	36
*Baringo[a]	8.8	47
*Baringo[b]	2.8	21
*Baringo N[c]	5.3	32
*Baringo S[c]	5.0	34
*Baringo[d]	7.6	40
♦Bogoria[e]	6.0	40
●Bogoria[a]	9.5	48
Olkaria wells	**$\delta^{18}O$ (‰)**	**δD (‰)**
*OW-703	4.5	34
*OW-705	3.7	25
*OW-706	2.2	21
*OW-715	1.0	4
*OW-2	2.1	3
*OW-5	3.7	18
*OW-16	3.1	10
*OW-21	2.8	8
*OW-22	2.7	13
*OW-23	3.6	13
*OW-26	2.6	11

Although H_2S/H_2 and CO_2/H_2 gas geothermometers from well MW-04 compare reasonably well (290-308°C), CO_2 geothermometer temperatures are significantly higher (320-332°C). Anomalously high CO_2 could be from a degassing magmatic heat source in Menengai, or reservoir fluid flashing. H_2S temperatures are higher than the solute geothermometer temperatures; this is considered to be a contribution of the well discharge from two feed zones, a deeper and hotter steam rich zone and a shallower, cooler water rich zone also inferred to in the temperature logs (Figure 13).

Two feed zones have been identified in well MW-04 (compared to four identified in MW-01 (Kipng´ok, 2011)) with one dominant feed zone at a depth of about 1700 m. A shallower feed zone of relatively low temperature is cased off at a depth of about 1050 m. The temperature and composition of the fluids at each feed zone is not known.

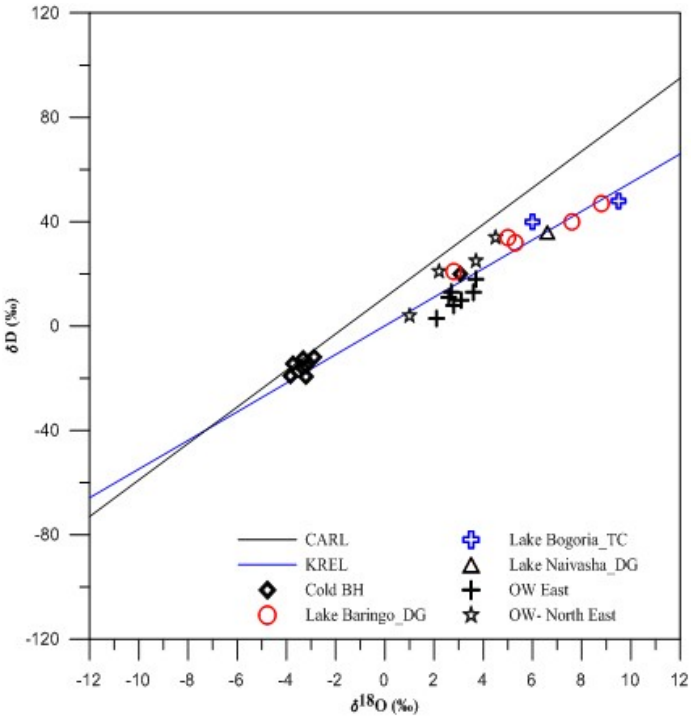

FIGURE 16: δD and $\delta^{18}O$ of all isotope data compiled. For comparison; the Kenya Rift Evaporation Line (KREL) and Continental African Rain Line (CARL) defined by Ármannsson (1994); previous Olkaria, Lake Baringo and Naivasha data by Darling (1996); Lake Bogoria data by Tiercelin and Vincens (1987), and Cioni et al. (1992)

Cold water inflow into the well is either increased or increased boiling is experienced during the change of the lip pressure pipe to smaller sizes. This phenomenon is shown on a plot of well head pressure (WHP) and an enthalpy in Appendix I (Figure 1) where the chloride concentration increases.

Although well MW-01 has discharged to a level which can be considered stable, erratic results likely indicate that the well might still be thermally unstable. It is important to note that well MW-04 had not reached thermal stabilization at the time this report was being written and, therefore, additional chemical data is required for good reservoir modelling.

The high bottom hole temperature, both during heat up and discharge in well MW-04, is most likely due to a non-porous layer below the lowest aquifer in the well. During drilling it got little cooling and is, therefore, fast to recover; this could also be inferred as a thin conductive layer below the well bottom with a high temperature gradient relative to the flow of fluids. During discharge the bottom section is not disturbed by the inflow above and therefore maintains a high temperature close to the formation temperature. Binocular analysis of well cuttings encountered at the well bottom infers a magmatic intrusion (Mibei, 2012).

Additional data is needed to entirely develop a model that would give a good prediction of the cold water inflow and the scaling potential.

7. CONCLUSIONS

The isotopic compositions of the lakes are enriched in ^{18}O and D compared to the wells, springs and cold shallow groundwater. They all follow closely the evaporation line defined by Ármannsson (1994). Because the lakes are shallow, their isotopic composition changes over time, depending on the rainfall patterns, lake levels and the amount of evaporation.

Very little isotopic variation is observed for the shallow cold groundwater (apart from the sample that is affected by Lake Naivasha) and it plots in a cluster on the $\delta^{18}O$ vs. δD diagram, slightly more positive than indicated by the intersection between the local rain water and the evaporation line.

Water from Menengai wells MW-01, MW-04 and MW-05 is a mixture of local groundwater and water from Lake Nakuru, at a ratio of 4:1, if the present isotope values for the lake are used. It is however difficult to give the exact mixing ratio because of the varying isotopic composition of the lake with time.

Higher oxygen shift is observed in well MW-05 due to water rock interaction at higher temperatures. It is, however, very important to measure the steam condensate from the well in order to be able to interpret the isotopic signature of the well.

There are significantly larger amounts of H_2S inflow into well MW-04 than into well MW-01; this could be an indication of steam heating of fluid in well MW-04.

Solute and gas geothermometer temperatures range from 150°C to 330°C, with the solute geothermometer temperatures being very low. The geothermometers show lower temperatures than the measured temperature in a discharging well. The temperature profile in Figure 12 shows the main inflow at 1600-1800 m depth, but no inflow of cooler water at shallower levels.

The waters discharged by wells MW-01 and MW-04 are mainly of sodium bicarbonate type, which according to Giggenbach (1991) are peripheral waters.

Calcite super saturation was observed from the fluid mineral equilibrium plot, with calcite scaling likely to occur in well MW-04.

ACKNOWLEDGEMENTS

I would like to thank my employer, Geothermal Development Company - GDC, for granting me the opportunity to attend this training programme. I am also grateful to Dr. Ingvar B. Fridleifsson, the director of the UNU Geothermal Training Programme, for offering me the chance to participate in this training programme, and to Mr. Lúdvík S. Georgsson, deputy director, for his successful organization of the programme. Many thanks go to my supervisors, Dr. Vigdís Hardardóttir and Prof. Árný Sveinbjörnsdóttir, for their good guidance, sharing of their knowledge and for supervision of this work. Many thanks also go to Mr. Gestur Gíslason, of Reykjavík Geothermal, for his assistance and knowledge. Sincere thanks to Ms. Thórhildur Ísberg, Ms. Málfrídur Ómarsdóttir, Mr. Ingimar G. Haraldsson and Mr. Markús A.G. Wilde, for their great help during the training period. I am grateful to the UNU-GTP 2012 Fellows for the wonderful time we have had together.

Special thanks to my family, and friends for their support, encouragement and prayers during my stay in Iceland. To my colleagues back in Kenya, thank you all for the support you extended to me. God bless you all.

Above all I want to thank the Almighty God for guiding me throughout the entire training period and for the opportunities that You continue to offer me and the ability and strength to get things done.

REFERENCES

Allen, D.J., and Darling, W.G., 1987: *Kenya Rift Valley geothermal project: Interpretation of fluid sample analyses from Magadi-Silali area.* British Geological Survey, Wallingford, U.K., 26 pp.

Allen, D.J., and Darling, W.G., 1992. *Geothermics and hydrology of the Kenya Rift Valley between Lake Baringo and Lake Turkana.* British Geological Survey, research report SD/92/1, 39 pp.

Allen D.J., Darling, W.G., Burgess, W.G., 1987: *Geothermics and hydrogeology of the southern part of the Kenya Rift Valley with emphasis on the Magadi-Nakuru area*. British Geological Survey, report SD/89/1, 68 pp.

Arnórsson, S., 1986: Chemistry of gases associated with geothermal activity and volcanism in Iceland. A review. *J. Geophys. Res., 91,* 12261-12268.

Arnórsson, S., 1998: *Practical uses of chemical geothermometers* (in Icelandic). Eyjar í eldhafi, Gott mál, Ltd., Reykjavík, 241-267.

Arnórsson, S., 2000a: The quartz and Na/K geothermometers. I. New thermodynamic calibration. *Proceedings of the World Geothermal Congress 2000, Kyushu-Tohoku, Japan,* 929-934.

Arnórsson, S., 2000b: The quartz and Na/K geothermometers. II. Results and application for monitoring studies. *Proceedings of the World Geothermal Congress 2000, Kyushu-Tohoku, Japan,* 935-940.

Arnórsson, S. (ed.), 2000c: *Isotopic and chemical techniques in geothermal exploration, development and use. Sampling methods, data handling, interpretation*. International Atomic Energy Agency, Vienna, 351 pp.

Arnórsson, S., Fridriksson, Th., and Gunnarsson, I., 1998: Gas chemistry of the Krafla geothermal field, Iceland. *Proceedings of the 9th International Symposium on Water-Rock Interaction 1998,* Balkema, Rotterdam, 613-616.

Arnórsson, S., and Gunnlaugsson, E., 1985: New gas geothermometers for geothermal exploration – calibration and application. *Geochim. Cosmochim. Acta, 49,* 1307-1325.

Arnórsson, S., Gunnlaugsson, E., and Svavarsson, H., 1983: The chemistry of geothermal waters in Iceland III. Chemical geothermometry in geothermal investigations. *Geochim. Cosmochim. Acta, 47*, 567-577.

Arnórsson, S., Sigurdsson, S. and Svavarsson, H., 1982: The chemistry of geothermal waters in Iceland I. Calculation of aqueous speciation from 0°C to 370°C. *Geochim. Cosmochim. Acta, 46,* 1513-1532.

Arnórsson, S., Stefánsson, A., and Bjarnason, J.Ö., 2007: Fluid-fluid interaction in geothermal systems. *Reviews in Mineralogy & Geochemistry*, *65,* 229-312.

Ármannsson, H., 1994: *Geothermal studies on three geothermal areas in West and Southwest Uganda.* UNDESD, UNDP project UGA/92/002, report, 85 pp.

Ármannsson, H., 2011: Application of geochemical methods in geothermal exploration. *Paper presented at "Short Course VI on Surface Exploration for Geothermal Resources", organized by UNU-GTP, GDC and KenGen, at Lake Naivasha, Kenya*, 8 pp.

Ármannsson, H., and Ólafsson, M., 2006: *Collection of geothermal fluids for chemical analysis*. ÍSOR – Iceland GeoSurvey, Reykjavík, report ISOR-2006/016, 17 pp.

Bigeleisen, J., 1952: The effects of isotopic substitutions on the rates of chemical reactions. *J. Phys. Chem., 56,* 823-828.

Bjarnason, J.Ö., 2010: *The speciation program WATCH, version 2.4.* ÍSOR – Iceland GeoSurvey, Reykjavík.

Can, I., 2002: A new improved Na/K geothermometer by artificial neural networks. *Geothermics, 31*, 751-760.

Cioni, R., Fanelli, G., Guidi, M., Kinyariro, J.K., and Marini, L., 1992: Lake Bogoria hot springs (Kenya): Geochemical features and geothermal implications. *J. Volcanology & Geothermal Research, 50,* 231-246.

Craig, H., 1961a: Standards for reporting concentrations of deuterium and oxygen-18 in natural waters. *Science, 133*, 1833-1834.

Craig, H., 1961b: Isotopic variations in meteoric water. *Science, 133*, 1702-1703.

Craig, H., 1963: The isotopic geochemistry of water and carbon in geothermal areas. In: Tongiorgi, E. (ed.), *Nuclear geology on geothermal areas*. Consiglio Nazionale delle Ricerche, Laboratorio di Geologia Nucleare, Pisa, 17-53.

D'Amore, F., 1991: Gas geochemistry as a link between geothermal exploration and exploitation. In: D'Amore, F. (coordinator), *Application of geochemistry in geothermal reservoir development* UNITAR/UNDP publication, Rome, 93-117.

Darling, W.G., Allen, D.J., and Ármannsson, H., 1990: Indirect detection of outflow from a Rift Valley Lake. *J. Hydrology., 113,* 297-305.

Darling, W.G., Gizaw, B. and Arusei, K.M, 1996: Lake-groundwater relationships and fluid rock interaction in the East African Rift Valley: Isotopic evidence. *J. African Earth Sciences, 22-4,* 423-431.

Dunkley, P.N., Smith, M., Allen, D.J., Darling, W.G., 1993: *The geothermal activity and geology of the northern sector of the Kenya Rift valley*. British Geological Survey, report SC/93/1, 185 pp.

Ellis, A.J., and Mahon, W.A.J., 1977: *Chemistry and geothermal systems*. Academic Press, NY, 392 pp.

Fournier, R.O., 1977: Chemical geothermometers and mixing model for geothermal systems. *Geothermics, 5,* 41-50.

Fournier, R.O., 1991: Water geothermometers applied to geothermal energy. In: D'Amore, F. (coordinator), *Application of geochemistry in geothermal reservoir development*. UNITAR/UNDP publication, Rome, 37-69.

Fournier, R.O., and Potter, R.W. II, 1982: A revised and expanded silica (quartz) geothermometer. *Geoth. Res. Council Bull., 11-10*, 3-12.

Fournier, R.O., and Truesdell, A.H., 1973: An empirical Na-K-Ca geothermometer for natural waters. *Geochim. Cosmochim. Acta*, *37*, 1255-1275.

Gat, J. R., 1996: Oxygen and hydrogen isotopes in the hydrologic cycle. *Annual Review. Earth Planet. Sci., 24,* 225-62.

GDC, 2012a: *Menengai isotope sampling locations map.* GDC, Kenya, database.

GDC, 2012b: *Menengai well locations map.* GDC, Kenya, database.

Giggenbach, W.F., 1988: Geothermal solute equilibria. Derivation of Na-K-Mg-Ca geoindicators. *Geochim. Cosmochim. Acta, 52*, 2749-2765.

Giggenbach, W.F., 1991: Chemical techniques in geothermal exploration. In: D'Amore, F. (coordinator), *Application of geochemistry in geothermal reservoir development*. UNITAR/UNDP publication, Rome, 119-144.

Kipng'ok, J.K., 2011: Fluid chemistry, feed zones and boiling in the first geothermal exploration well at Menegai, Kenya. Report 15 in: *Geothermal training in Iceland 2011*. UNU-GTP, Iceland, 281-302.

Lagat, J., Mbia, P., and Mutria, C., 2010: *Menengai prospect: Investigations for its geothermal potential.* GDC, Kenya, internal report, 64 pp.

Mibei, G.K., 2012: Borehole geology and hydrothermal alteration of Menengai geothermal field. Case study: wells MW-04 and MW-05. Report 21 in: *Geothermal training in Iceland 2012.* UNU-GTP, Iceland, 437-466 pp.

Mungania, J., 2004: *Geological studies of Menengai geothermal prospect*. KenGen, Ltd., Kenya, internal report, 18 pp.

Nehring, N.L., and D`Amore, F., 1984: Gas chemistry and thermometry of the Cerro Prieto, Mexico, geothermal field. *Geothermics, 13*, 75-89.

Nicholson, K., 1993: *Geothermal fluids: chemistry and exploration techniques*. Springer-Verlag, Berlin, 268 pp.

Simiyu, S.M., and Keller, G.R., 1997: An integrated analysis of the lithospheric structure across the East African plateau based on gravity analysis and recent seismic studies. *Tectonophysics, 278,* 291-313.

Simiyu, S.M., and Keller, G.R., 2001: Geophysical interpretation of the upper crustal structure of the southern Kenya rift. *Geophys. J. Internat., 1245*, 234-267.

Sveinbjörnsdóttir, Á.E., Johnsen, S.J., Kristmannsdóttir H., and Ármannsson, H., 2004: Isotopic characteristic of natural waters in the Southern Lowlands of Iceland. *Proceedings of the 11th International Symposium on Water-Rock Interaction 2004, New York, USA*. Taylor & Francis Group, London, 1404-1405.

Tiercelin, J.J., and Vincens, A. (eds.) 1987: Le demi–graben de Baringo–Bogoria, Rift Gregory, Kenya: 30,000 ans d'histoire hydrologique et sédimentaire (in French). *Bulletin des Centres de Recherches Exploration-Production Elf-Aquitaine, 11*, 249-540.

Tole, M.P., Ármannsson, H., Pang Z.H., and Arnórsson, S., 1993: Fluid/mineral equilibrium calculations for geothermal fluids and chemical geothermometry. *Geothermics, 22*, 17-37.

Urey, H.C., 1947: The thermodynamic properties of isotopic substances. *J. Chem. Soc.,* 562–581.

APPENDIX I: Well MW-04, change in Cl concentrations with lip pressure

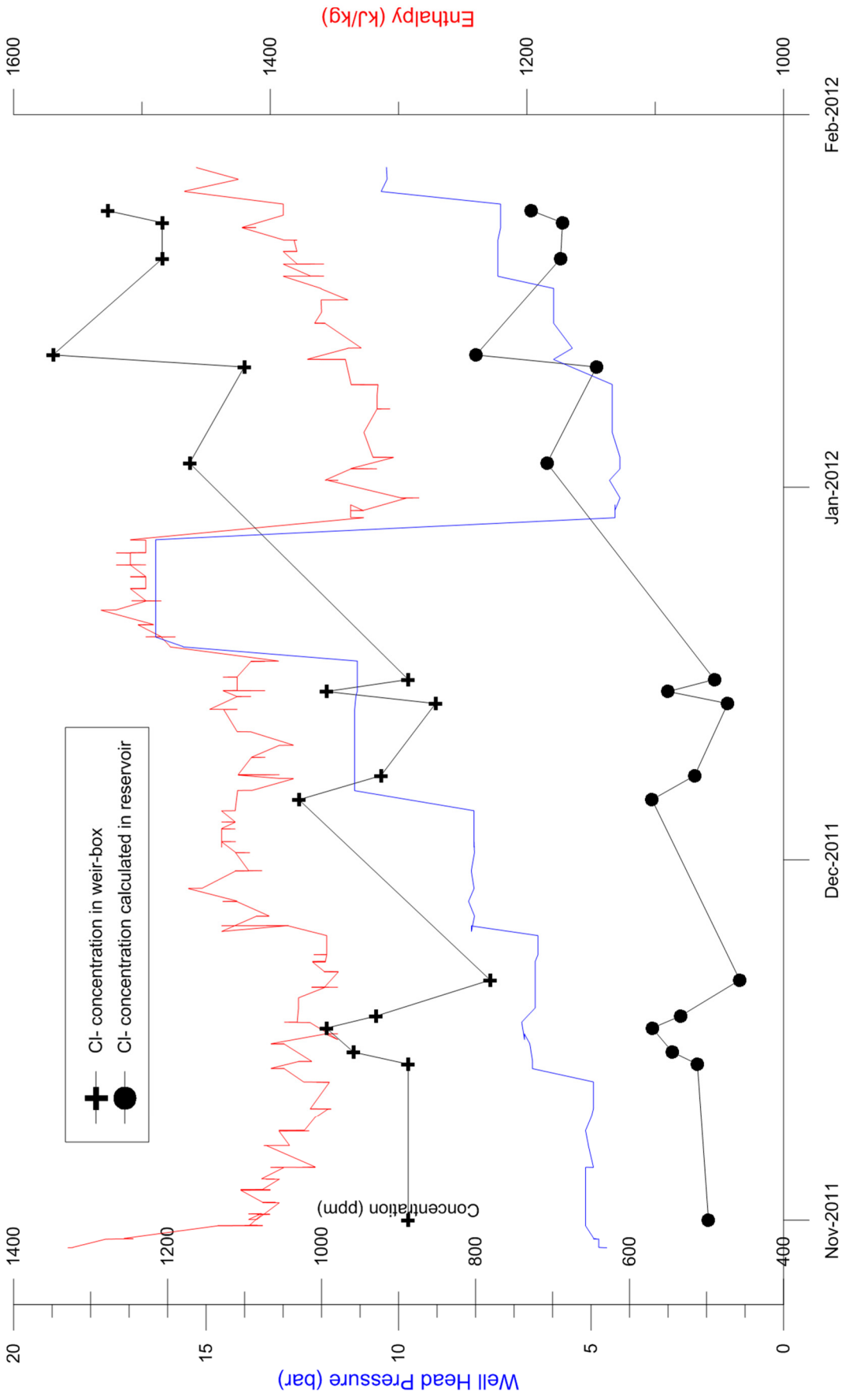

FIGURE 1: Change in Cl concentrations with change in lip pressure pipe in Menengai well MW-04